

The Relation between Laser-Induced Chlorophyll Fluorescence and Photosynthesis

A. Rosema,* J. F. H. Snel,[†] H. Zahn,* W. F. Buurmeijer,[†]
and L. W. A. Van Hove[‡]

The remote sensing literature on laser-induced chlorophyll fluorescence has indicated a relation between chlorophyll fluorescence and photosynthesis but, so far, has not presented a quantitative interpretation of the measurements. The present article presents the development of a model to quantify the gross photosynthesis on the basis of remote measurements of chlorophyll fluorescence and radiance with the Laser Environmental Active Fluorosensor (LEAF-NL). Combined measurements of the laser-induced chlorophyll fluorescence and CO₂ exchange have been carried out during several days. Drought and ozone stress were imposed in two separate experiments. The laser-induced fluorescence measurements show a remarkable behavior. After sunrise the fluorescence yield rises first, but at high radiation and high temperature the fluorescence yield may decline below the nighttime fluorescence. This extremely strong quenching of fluorescence is attributed to photosystem deactivation. On the basis of the available laser-induced fluorescence data, a photosystem energy partitioning model is developed and finally used to predict photosynthetic electron transport. The results of this new model are compared with those of the current theory and with the CO₂ assimilation data. Contrary to the current theory, the results from the new model show a fairly good correspondence with the CO₂ assimilation data. It is believed that the present results are a significant step forward to the development of practical applications. ©Elsevier Science Inc., 1998

INTRODUCTION

During the past decade there have been several research programs in the field of laser-induced fluorescence of plants (Günther et al., 1991, 1994; Lichtenthaler et al., 1992; Stober et al., 1994; Methy et al., 1994; Schmuck and Moya, 1994; Lipucci di Paola et al., 1992; Rosema et al., 1988, 1992, 1994a,b; Cecchi et al., 1994; Valentini et al., 1994). An issue of this journal was largely dedicated to this relatively new class of remote sensing techniques (*Remote Sens. Environ.* 47, 1994). The present article only addresses the laser-induced fluorescence of plant chlorophyll, which occurs in the red and near-infrared wavelength range with maxima at 685 nm and 730 nm. It is known that this dynamic signal is related to the light reaction of photosynthesis. Its quantitative interpretation in terms of photosynthesis is a major challenge and would greatly stimulate the practical application of this type of remote sensing.

Articles on laser-induced chlorophyll fluorescence have usually focused on the fluorescence band ratio (FBR = F_{730}/F_{685}) mainly with the argument that this would "normalize" the signal. We have shown in earlier publications (Rosema et al., 1991; Rosema and Verhoef, 1991) that the FBR depends on optical properties such as excitation wavelength, chlorophyll amount, leaf area index, leaf orientation, and background reflection. It was shown that the ratio of 690 nm and 770 nm reflection is much more sensitive to variations in chlorophyll content than the FBR (Rosema and Verhoef, 1991). With this approach it is difficult to see what more laser-induced chlorophyll fluorescence techniques could offer than spectral reflection measurements.

The photosynthesis information is present in the absolute values of the chlorophyll fluorescence and is in fact completely or largely eliminated when taking the fluorescence band ratio. Already in 1980s it was found that the laser-induced fluorescence signal showed strong daily

* EARS Remote Sensing Consultants, Delft, The Netherlands

[†] Agricultural University of Wageningen, Department of Plant Physiology, Wageningen, The Netherlands

[‡] Agricultural University of Wageningen, Department of Air Pollution, Wageningen, The Netherlands

Address correspondence to A. Rosema, EARS Remote Sensing Consultants, P.O. Box 449, 2600 AK Delft, The Netherlands. E-mail: ears.delft@inter.nl.net

Received 19 June 1997; revised 9 January 1998.

variations, which seemed to be related to effects of air pollution on photosynthesis, but were not really understood (Rosema et al., 1988). During the 1990s we have therefore focused our research on the explanation of the daily course of the laser-induced fluorescence signal and its relation to photosynthesis. The present article presents a detailed model to quantify the gross photosynthesis on the basis of remote measurements of chlorophyll fluorescence and radiance with a single instrument in a single wavelength band. The model is derived on the basis of actual measurements during a number of days. A modification of existing theory of photosynthetic electron transport appeared necessary to explain the peculiar behavior of the changes in fluorescence that occur during the day. The knowledge obtained and the model developed is expected to be very useful for the planning of data acquisition and the interpretation chlorophyll fluorescence data obtained by remote sensing.

The plant physiological literature provides an abundance of information on the subject of chlorophyll fluorescence, including models which could provide a quantitative relation between fluorescence and photosynthetic electron transport. Much of the results in this field, however, are based on the use of chlorophyll fluorometers at the level of single leaves. An overview of such instruments has been presented by Mohammed et al. (1995). These instruments use an "analytic" light source ($\leq 1 \mu\text{mol}/\text{m}^2 \text{ s}$) for excitation. The weak excitation light does not notably affect the photosynthetic state of the plant. The more advanced instruments make use of a modulated light source and synchronic detection of the fluorescence signal. This allows measurement of the fluorescence yield in daylight (ϕ'_F). An additional saturating light pulse of about 1 s is used to close all reaction centers. In this way the maximum fluorescence yield is obtained (ϕ'_{FM}). These two measurements then enable the calculation of the photosynthetic quantum yield (ϕ'_P), as shown by Genty et al. (1989):

$$\phi'_P = 1 - \phi'_F / \phi'_{FM} \quad (1)$$

In an earlier article in this journal (Rosema and Zahn, 1997) the question was raised whether laser-induced fluorescence measurements can be interpreted in the same way as chlorophyll fluorometer measurements. Because of the high light intensity of the excitation source, that is, the laser pulse, there is a risk that the state of the photosynthetic system is affected due to reaction center closure or exciton annihilation. By means of theoretical modeling and actual measurements with the Laser Environmental Active Fluorosensor (LEAF-NL), we have shown that such unwanted effects do not occur, provided that the laser excitation energy does not exceed $100 \text{ mJ}/\text{m}^2$.

In the present article the interpretation of the laser-induced fluorescence signal in terms of photosynthesis is considered. To this end, laser-induced fluorescence and CO_2 assimilation measurements have simultaneously been carried out on young poplar trees.

EXPERIMENTAL SET-UP

Growing of Plant Material

Poplar (*Populus nigra* Brandaris) cuttings were prepared and incubated for rooting as described by Pieters and Van den Noort (1985). After rooting, the plants were grown in a phytotron room at 20°C , 70% relative humidity, and $55 \text{ W}/\text{m}^2$ ambient light, with a day length of 16 h. At night the conditions were 18°C and 60% relative humidity. Plants with a length of approximately 80 cm were selected for the measurements.

The plants were placed in a growth cabinet with glass walls, functioning as an open gas exchange system (Van Hove, 1989). The growth cabinet was located within a greenhouse (UNIFARM, Wageningen Agricultural University), allowing the plants to be subjected to normal day-light cycles.

CO_2 Assimilation

Figure 1 illustrates the setup used for the gas exchange measurements. Ambient air was pumped through the cabinet via a buffer to reduce fluctuations in air pressure. The data from the CO_2 analysers were corrected for air pressure fluctuations (measured with a Multur AD 1000 absolute pressure sensor, Halstrup Multur, Erwin, Germany) and variations in the water vapor pressure. The average air flow through the cabinet was set to about $0.006 \text{ m}^3/\text{s}$ and was continuously monitored using a differential pressure sensor (Delta-P P4, Halstrup Multur, Erwin, Germany). The selection of the measuring points for the various analysers was under control of a WA 161 MK3 channel selector (ADC, Hoddesdon, United Kingdom), with a full sampling cycle through all six channels of about 15 min. Four channels were used to sample the inlet and the outlet of the air flowing through the cabinet. The remaining two channels served as control enabling the correction for zero drift of the water vapor monitor (ADC 225 MK3 Water Vapour mB, ADC, Hoddesdon, United Kingdom) and the absolute CO_2 monitor (BINOS 1, Leybold-Heraeus, Woerden, Netherlands). To increase the sensitivity at low photosynthetic activity, a differential CO_2 monitor (ADC 225 MK3, ADC, Hoddesdon, United Kingdom) was used in addition to measure the difference between the inlet and outlet air directly. Since two channels were used to sample both the inlet and outlet, the effective acquisition time step was 7–8 min.

Drought and Ozone Stress

Two types of stress were imposed on the plants. Ozone stress was induced by the injection of ozone enriched air from an ozone generator (Fischer Model 500, Fischer, Bonn, Germany) just before the buffer. The ozone concentration was measured with an ozone monitor (Mon Labs 8810, Monitor Labs, San Diego, USA). During ozone fumigation the average concentration of the outgoing air was approximately $400 \mu\text{g}/\text{m}^3$. When ozone fumiga-

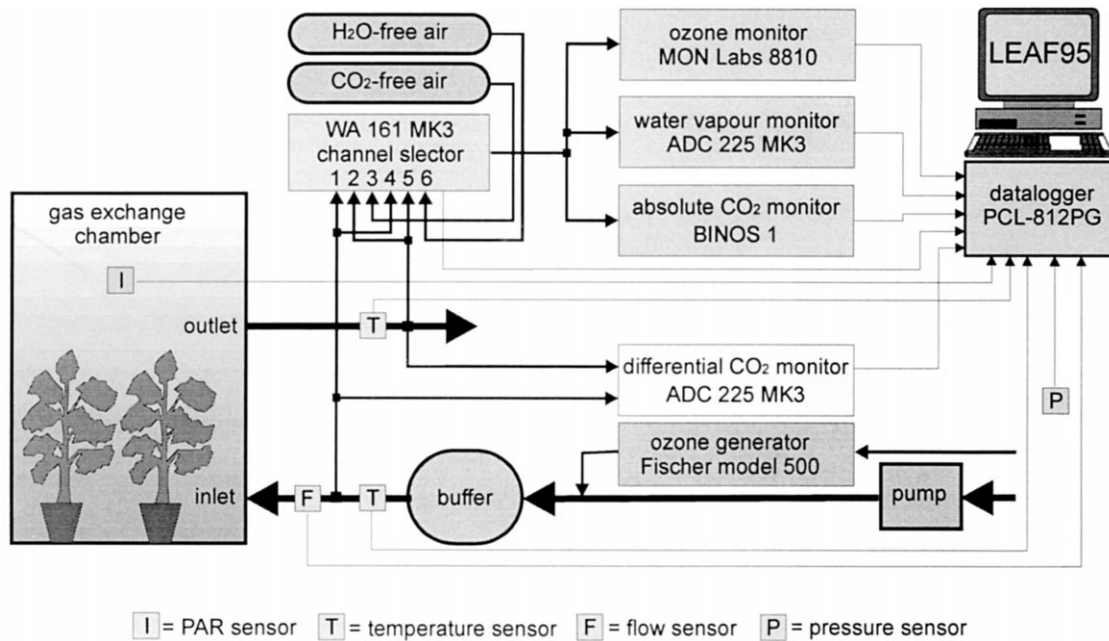


Figure 1. Setup used to monitor the net CO₂ assimilation of poplar trees.

tion was applied, the outlet of the main air stream was placed outside the greenhouse to avoid contamination of the inlet air.

Drought stress was induced by gradual drying of the plant pots after watering at the beginning of the experiment. The data were digitized and stored using dedicated software running on a 386SX/25 PC equipped with an Advantech PCI-812PG Labcard IO-board (Advantech Benelux, Roosendaal, Netherlands).

Laser-Induced Chlorophyll Fluorescence Measurements

Laser-induced fluorescence measurements were carried out with the Laser Environmental Active Fluorosensor (LEAF-NL) on the poplar plants inside the growth cabinet along a horizontal optical path through the glass walls of the cabinet. To avoid that the growth of leaves would influence the signal, the field of view of the LEAF-NL instrument did not include the plant tops.

The Nd-Yag laser of the LEAF-NL instrument provides 10 mJ pulses of 10 ns length at 532 nm wavelength. The measuring distance to the cabinet was 12 m. The divergence of the laser beam was chosen 50 mrad and so the diameter of the laser spot hitting the plants leaves was approximately 60 cm. The corresponding pulse energy density was about 50 mJ/s, that is, sufficiently low to prevent disturbing effects that could result from reaction center closure and exciton annihilation. Interpretation of the laser-induced fluorescence data along the theoretical lines developed in chlorophyll fluorometry is therefore justified (Rosema and Zahn, 1997).

The LEAF-NL instrument measures the scene ra-

diance with and without laser excitation in four wavelength bands (Rosema et al., 1994b). The laser-induced fluorescence is the difference between the active signal (measured with the laser pulse) and the passive signal (measured without the laser pulse). The chlorophyll fluorescence spectrum has two maxima at 685 nm and 730 nm, respectively. The fluorescence has been measured in two 20 nm wide spectral bands, which were centered at these two wavelengths, respectively.

The passive signal in the 730 nm band was used to estimate the variable PAR level on the plant leaves as observed with the LEAF-NL instrument. This was done by regression between the 730 nm band counts and the PAR values measured inside the cabinet.

Fluorometer Measurements

In a supplementary experiment measurements were done with the EARS Plant Photosynthesis Meter (EARS-PPM, EARS, Delft, Netherlands), a hand-held chlorophyll fluorometer. It uses a 7200 Hz modulated LED at 637 nm for excitation, with a 690 nm infrared cutoff filter in front. Chlorophyll fluorescence, after passing through a 700 nm infrared transmitting filter, is measured synchronically by means of a PIN Si photodiode, preamplifier, automatic gain control, synchronic detector, and low-pass electronic filter. A 6-V, 15-W Halogen lamp with near-infrared blocking filter in front is used to generate a 5000 $\mu\text{mol}/\text{m}^2 \text{ s}$ saturating light pulse, capable of closing all photosystem reaction centers. The duration of this light pulse is automatically determined from the course of the chlorophyll fluorescence signal and is usually between 0.5 s and 1 s.

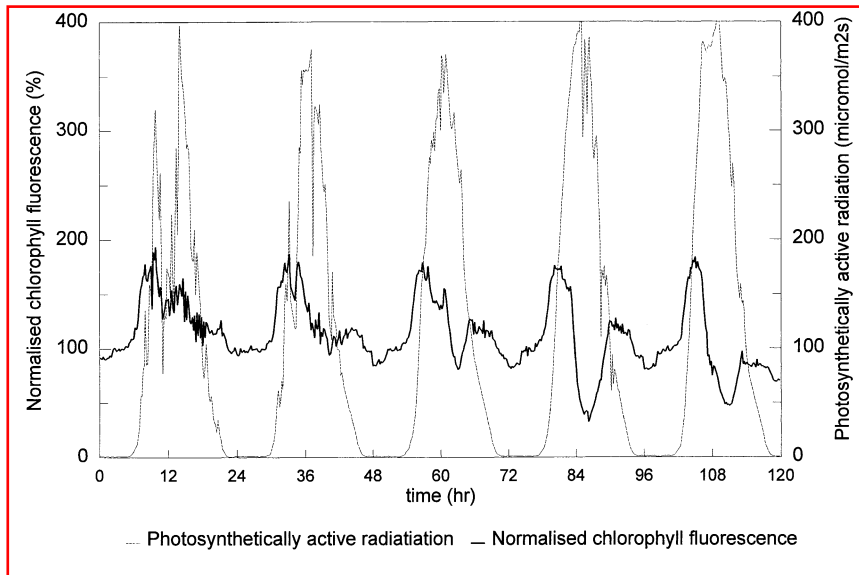


Figure 2. Fluorescence at 730 nm and PAR measured on the poplar trees with the Laser Environmental Active Fluorosensor (LEAF-NL) during the drought experiment. The fluorescence is normalized to the pre-dawn values and expressed in %. Note the afternoon decline of the fluorescence far below the nighttime level.

With the PPM two fluorescence yield measurements are carried out: one under ambient light (ϕ_f') and one after closing all reaction centers with the saturating pulse (ϕ_{FM}'). From these the yield of photochemistry (ϕ_f) is calculated with Eq. (1). In addition the PPM measures the photosynthetically active radiation (PAR) incident on the plant leaf by means of a blue enhanced Si photodiode with a 400–690 nm transmitting filter, which is measuring the light scattered from a white diffusor next to the leaf.

RESULTS

Description of the Laser-Induced Fluorescence Measurements

Figure 2 shows the time course of the laser-induced fluorescence signal measured in the 730 nm band and the corresponding PAR level during 5 days of the drought experiment. The fluorescence signal has been normalized relative to the predawn fluorescence value and is therefore expressed in percent. Only the 730 nm fluorescence signal is shown as there appeared to be no significant difference between the 685 nm and 730 nm fluorescence signal. The fluorescence band ratio ($FBR = F_{685}/F_{730}$) varied only 20%, in spite of the dramatic fluorescence changes that occurred during the daily cycle. Variations between 40% and 180% of the predawn fluorescence value were observed, as shown in Figure 2.

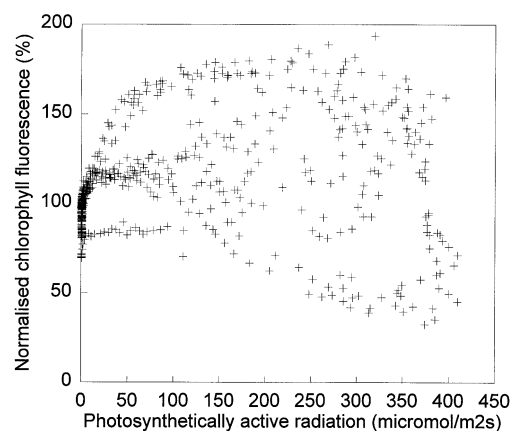
The PAR level during the drought experiment varied between 0 and 400 $\mu\text{mol}/\text{m}^2 \text{ s}$. The first daily period in the graph represents the reference day (20 June) when the plant was still well supplied with water. Thereafter the plants were left without water supply. The following daily periods are those of 26–29 June.

Figure 3 shows a scattergram of the normalized 730 nm fluorescence signal versus the simultaneous PAR level. The fluorescence data presented in both Figures 2

and 3 demonstrate a very typical, periodic behavior. The following phenomena are observed.

1. On the first, reference day, the chlorophyll fluorescence more or less follows the changes in the PAR level, although PAR is distributed more symmetrically around noon. The fluorescence distribution is skew and shows higher values in the morning than in the afternoon.
2. The maximum fluorescence occurs halfway through the morning between 9:00 a.m. and 9:30 a.m., when PAR is about 180 $\mu\text{mol}/\text{m}^2 \text{ s}$. The maximum value reached is about 1.8 times the predawn fluorescence value. At higher PAR levels the fluorescence decreases.
3. On later days, when drought stress develops more

Figure 3. Scattergram of the laser-induced fluorescence versus PAR taken during the drought experiment. Note the hyperbolic upper part of the data, which is passed through during the early morning. Thereafter the fluorescence tends to decline.



and more, the skewness of the fluorescence distribution around noon becomes more pronounced and a slump in the fluorescence develops during the afternoon. The time elapsed between the radiation maximum and the fluorescence slump is about 3 h. The lowest fluorescence value during the slump is only 40% of the predawn fluorescence level. In the ozone experiment values as low as 10% were observed.

4. In the later afternoon the fluorescence value restores, but after sunset is still lower than the predawn value. During the night the fluorescence value gradually rises to the predawn level in a period of about 4 h.

The behavior of the daily fluorescence cycle is rather unexpected in view of results obtained with single leaves by Srivastava et al. (1995). Particularly, the reduction of the noon fluorescence to levels far below the fluorescence yield in the dark is remarkable. There seem to be two regulating mechanisms that are both induced by solar radiation but at different time scales. The first mechanism is an immediate positive effect of radiation on the fluorescence, which, however, saturates at higher radiation levels (Fig. 3, upper branch of data). This is attributed to reaction center closure in combination with increased dissipation of excitation energy at higher light levels. The second mechanism dramatically reduces the fluorescence yield to a level far below the predawn fluorescence level, which is assumed to correspond to fully open reaction centers (φ_{F0}). This effect seems to be related to high radiation levels but is delayed in phase by several hours. Comparison with CO₂ exchange data indicates that this mechanism occurs simultaneously with a strong decrease in CO₂ assimilation as will be shown later (Fig. 10). The phenomenon of a strong decrease in fluorescence under high radiation is also present, but not explained, in the laser-induced fluorescence data presented by Moya et al. (1995). In the following section we will briefly discuss the current theory of photosystem energy partitioning so as to be able to explain the experimental results.

Photosystem Energy Partitioning

The photosynthetic reaction takes place in photosystems (PS) which consist of an antenna or "light harvesting complex" (LHC) connected to a reaction center (RC). There are two kinds of photosystems, PSII and PSI, which work serially together. The photosystems are embedded in a membrane of lipids and proteins, the thylakoid. The *in vivo* chlorophyll fluorescence originates mainly from PSII. When a photon is captured by its antenna, an electron is transferred into the excited state. This "exciton" travels randomly through the antenna and may lose its energy by several competing reactions. The main possibilities are:

1. The exciton is absorbed by the reaction center and used for photochemistry.
2. The surplus energy of the electron is dissipated into heat by collision.
3. The surplus energy of the electron is emitted as a photon (fluorescence).

Each possibility has a specific probability, which is expressed in the corresponding rate constant: k_P for photochemistry, k'_D for dissipation, and k_F for fluorescence emission. The rate constant for dissipation k'_D is known to increase with increasing light level (e.g., Srivastava et al., 1995). Its lowest value, at dark, is denoted k_D . The two are arbitrarily related by

$$k'_D = \alpha k_D. \quad (2)$$

The deexcitation reactions takes place on very short time scales in the order of 10^{-9} s. Once a reaction center has absorbed an exciton, it remains closed for a relatively long period in the order of 10^{-4} s.

The energy partitioning model used by Genty et al. (1989) assumes separate photosystems. Two populations are discerned: open systems and closed systems. The yields of the different deexcitation reactions are found from the ratio between the relevant rate constant and the sum of all rate constants. For open systems, the fluorescence yield and the photochemical yield are then given by

$$\varphi'_{F0} = k_F / (k_F + k'_D + k_P), \quad (3)$$

$$\varphi'_{P0} = k_P / (k_F + k'_D + k_P). \quad (4)$$

Closed systems are not capable of photochemistry and thus have only two possibilities for deexcitation (k_F and k'_D). While the photochemical yield is zero, the fluorescence yield of closed systems is given by

$$\varphi'_{FM} = k_F / (k_F + k'_D). \quad (5)$$

If the fraction of open systems is u , the overall yields of fluorescence and photochemistry are given as follows:

$$\varphi'_F = u \cdot k_F / (k_F + k'_D + k_P) + (1 - u) \cdot k_F / (k_F + k'_D), \quad (6)$$

$$\varphi'_P = u \cdot k_P / (k_F + k'_D + k_P). \quad (7)$$

In these equations the nomenclature proposed by Van Kooten and Snel (1990) is followed. The prime in φ'_F and φ'_P denotes yields that are affected by increased energy dissipation ($\alpha > 1$) or "nonphotochemical quenching." The apostrophe is omitted if $\alpha = 1$, that is, at dark or very low light.

A relation between the quantum yield of fluorescence and the quantum yield of photosynthesis is obtained by eliminating the fraction of open systems (u) from Eqs. (6) and (7). With the appropriate substitutions, this leads to the earlier mentioned relation of Genty et al. (1989), which reads

$$\varphi'_P = 1 - \varphi'_F / \varphi'_{FM}. \quad (8)$$

This equation has been widely used to determine the photosynthetic quantum yield by means of fluorimeters that apply a modulated excitation source and a strong additional light pulse to close all photosystems, such as the WALZ-PAM and the EARS-PPM.

Photosynthetic Yield as a Function of PAR

The relationship between photosynthesis and PAR has been described by many mathematical functions, including the hyperbolic function (e.g., Poulet et al., 1983). The hyperbolic relation suggests that the photosynthetic quantum yield (ϕ_p') is also a hyperbolic function of PAR. A useful explanation of this hyperbolic relationship might be found in considering exciton delivery (E_l) to the reaction centers (the "light reaction") and electron transport (E_d) from the reaction centers into the photosynthetic system (the "dark reaction") separately.

The light reaction is proportional to the number of open photosystems (u) and can be expressed as

$$E_l = \phi_p' \cdot \text{PAR} = u \cdot \phi_{p0}' \cdot \text{PAR}. \quad (9)$$

This is not the case with the dark reaction. On the contrary, if all reaction centers are open ($u=1$) the dark reaction cannot take place. Electron transport (E_d) into the photosynthetic system will be proportional to the number of closed photosystems ($1-u$). We will assume that an electron transport resistance r_e is involved. The electron transport (i.e., reopening of the closed PSII reaction center) may then be formulated as follows:

$$E_d = (1-u)/r_e. \quad (10)$$

On time scales of milliseconds and longer there must exist equilibrium between exciton delivery to the reaction centers (E_l) and transport of electrons away from the reaction centers (E_d), and thus $E_l = E_d = E$. A relation between the photosynthetic yield and the light level may then be found by eliminating u from Eq. (9) and Eq. (10). This leads to

$$E = \phi_{p0}' \cdot \text{PAR} / (1 + r_e \cdot \phi_{p0}' \cdot \text{PAR}), \quad (11)$$

or, since $\phi_p' = E/\text{PAR}$,

$$\phi_p' = \phi_{p0}' / (1 + r_e \cdot \phi_{p0}' \cdot \text{PAR}). \quad (12)$$

This equation predicts the quantum yield of photosynthesis to be a hyperbolic function of the photosynthetic active radiation (PAR).

Fluorescence Yield as a Function of PAR

By substitution of ϕ_p' (12) in (8), also the fluorescence yield may be expressed as a function of PAR:

$$\phi_F' = \phi_{FM}' (1 - \phi_p') = \phi_{FM}' [1 - \phi_{p0}' / (1 + r_e \cdot \phi_{p0}' \cdot \text{PAR})]. \quad (13)$$

Since the LEAF-NL laser-induced fluorescence yield measurement is not calibrated, it is useful to normalize the fluorescence yield to a reference level. For this purpose it is divided by the fluorescence yield of the fully

dark adapted photosystems (ϕ_{F0}). This reference value is easily measured and in the case of the laser-induced fluorescence measurements is supposed to exist just before dawn. Thus one obtains

$$\phi_F' / \phi_{F0}' = (\phi_{FM}' / \phi_{F0}') [1 - \phi_{p0}' / (1 + r_e \cdot \phi_{p0}' \cdot \text{PAR})]. \quad (14)$$

From Eq. (8) we find for open reaction centers $\phi_{FM}' = \phi_{F0}' / (1 - \phi_{p0}')$, and this is used to substitute ϕ_{FM}' in Eq. (14). In addition we may derive from Eqs. (2) and (3) that $\phi_{F0}' / \phi_{F0} = \phi_{p0}' / \phi_{p0}$. In this way (14) is expressed in terms of the photochemical yields of open reaction centers only:

$$\phi_F' / \phi_{F0}' = \{ \phi_{p0}' / [(1 - \phi_{p0}') \phi_{p0}] \} [1 - \phi_{p0}' / (1 + r_e \cdot \phi_{p0}' \cdot \text{PAR})]. \quad (15)$$

The photochemical yield of open reaction centers, however, still depends on the rate of energy dissipation k'_b , that is, on a . Using Eqs. (2), (3), and (4), the following expression of ϕ_{p0}' in terms of a and ϕ_{p0} may be obtained:

$$\phi_{p0}' = \phi_{p0} / [1 + (a-1)(1 - \phi_{p0} - \phi_{F0})]. \quad (16)$$

With (15) substituted in (14), the normalized fluorescence yield is entirely expressed in terms of the fully dark adapted yields (ϕ_{p0} and ϕ_{F0}), the rate of energy dissipation (a), the electron transport resistance (r_e), and the photosynthetic active radiation level (PAR). This substitution, however, will not be shown here because of the complexity of the expression that is obtained. The values of the fully dark adapted yields, ϕ_{p0} and ϕ_{F0} , are fairly well known. Demmig and Björkman (1987) have shown that for both C3 and C4 plants $\phi_{p0} \cong 0.82$. ϕ_{F0} is small, about 0.01. Thus Eqs. (15) and (16) express the chlorophyll fluorescence yield in terms of three unknowns: PAR, a and r_e . The electron transport resistance r_e is assumed to be a constant. This, however, is not the case for a , which represents the increase of energy dissipation at higher light levels. In several cases an approximately linear relationship was found between nonphotochemical quenching of the fluorescence and PAR in plants adapted to high light (Björkman and Demmig-Adams, 1995). As a first approximation we will therefore assume a linear relation between a and the photosynthetic active radiation:

$$a = 1 + b \cdot \text{PAR}. \quad (17)$$

Substituting this in Eq. (16), the following expression is obtained

$$\phi_{p0}' = \phi_{p0} / [1 + b \cdot \text{PAR} \cdot (1 - \phi_{p0} - \phi_{F0})]. \quad (18)$$

With Eqs. (15) and (18) the behavior of the normalized fluorescence yield as a function of PAR, with r_e and b as parameters, can be simulated. The effect of various values for b and r_e is shown in Figures 4 and 5, respectively. If we compare these with the observations shown in Figure 3, it appears impossible to explain all observations in this way. It is possible, however, to obtain a good fit with the upper part of the fluorescence yield data shown in this figure, which represent the fluorescence values mea-

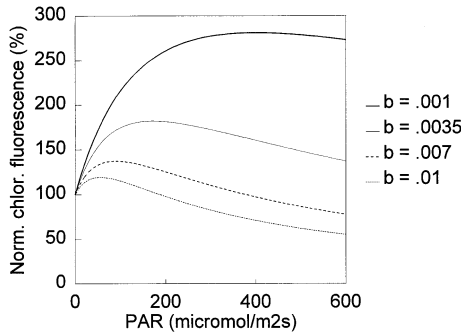


Figure 4. Theoretical calculation of the normalized chlorophyll fluorescence yield as a function of PAR for various values of the heat dissipation constant b .

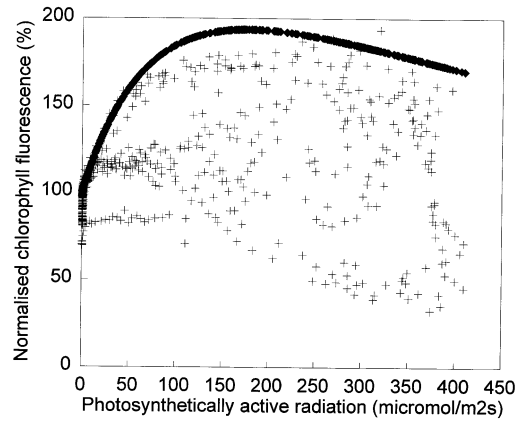


Figure 6. Scattergram of the laser-induced fluorescence versus PAR. The modeled function, applying to active photosystems only, is shown superimposed. The decline of the fluorescence below this function is assigned to photosystem deactivation.

sured during the morning at relatively low radiation. This fit, shown in Figure 6, is obtained for the following values of the constants involved:

$$r_e = 0.005, \quad (19)$$

$$b = 0.0035. \quad (20)$$

The other strongly quenched fluorescence values plotted in this graph, which do not fit the hyperbolic relation, correspond to high radiation levels.

Nature of Strong Fluorescence Quenching under High Radiation

It might be argued that the strong decline in fluorescence is not caused by a lowered fluorescence yield but by a decreased light absorption and/or changes in canopy structure. Visually, however, no reflectivity changes were observed. The following experiment indicates that also canopy structure is not involved. Figures 7 and 8 show measurements on a *Ficus robusta* plant, placed outdoor on a sunny and a cloudy summer day, respectively. The

fluorescence measurements were done with the PPM modulated fluorometer on a single leaf. Figure 7 shows the time course of the fluorescence and PAR. In the afternoon of the first, sunny day an enormous decline in the fluorescence is taking place. This apparently is the same phenomenon as observed in the laser-induced fluorescence measurements on poplar. This slump in the fluorescence does not occur during the second, cloudy day. Figure 8 shows a plot of the fluorescence yield values versus the simultaneous values of the photochemical yield for these two days. It appears that most of the measurements lie on a straight line, except those corresponding to the fluorescence slump under high light. For these data there appears to be no unique relation between ϕ_F' and ϕ_F' . On the contrary, strong hysteresis occurs.

The strong quenching of the fluorescence under high radiation might be the result of enhanced dissipation of excitation energy. This could be caused by i) dissipation in the PSII reaction center, ii) dissipation in the

Figure 5. Theoretical calculation of the normalized chlorophyll fluorescence yield as a function of PAR for various values of the effective electron transport resistance r_e . The combination $b=0.0035$ and $r_e=0.005$ gives a good correspondence with the upper part of the observed data in Figure 3.

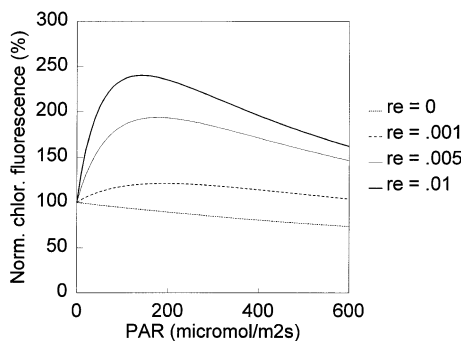
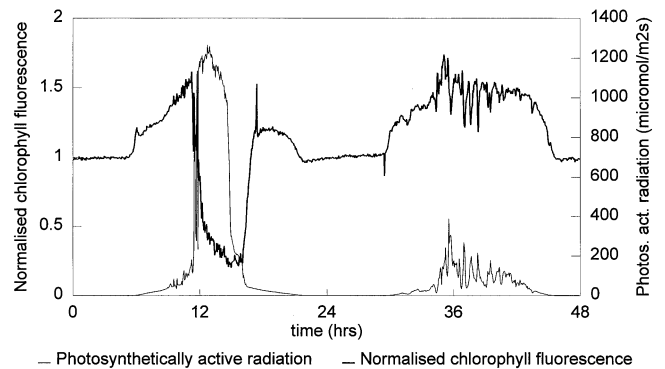


Figure 7. Normalized chlorophyll fluorescence (ϕ_F'/ϕ_{F0}) and PAR, measured with the PPM on *Ficus robusta*, as a function of time, on a sunny and a cloudy day, respectively.



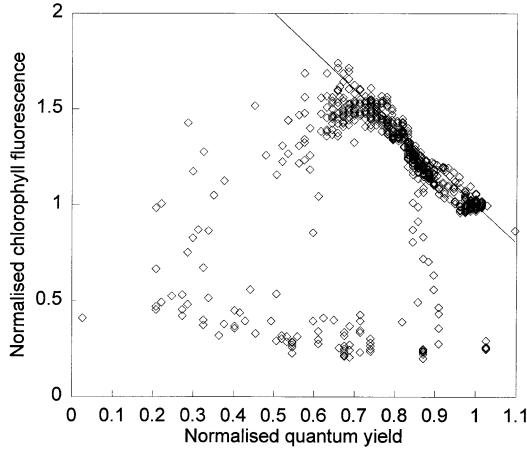


Figure 8. Scattergram of the normalized chlorophyll fluorescence (ϕ'_p/ϕ_{p0}) versus the normalized photochemical quantum yield (ϕ'_p/ϕ_{p0}). Early morning data at low radiation are linearly related. Strongly quenched noon data, taken under high radiation, show strong hysteresis.

antenna, or iii) disconnection of (a part of) the antenna from the reaction center. It should be noted, however, that the mechanism of dissipation in the reaction center cannot be related to photoinhibition as the fluorescence yield during the slump is much lower than the fluorescence yield in the dark. The mechanism of dissipation in the antenna requires an increase of a during the day, suggesting that the relation between a and PAR is variable. Leaf temperature has been shown to affect zeaxanthin formation and non-photochemical quenching (Bilger and Björkman, 1991). Temperature was also shown to affect aggregation and fluorescence emission of isolated LHCII in vitro (Bardza et al., 1996).

Although it is not clear which mechanism is involved, it is obvious that, under conditions where a linear relationship between ϕ'_p and ϕ'_F exists, chlorophyll fluorescence can be used to estimate photosynthetic electron flow. As under high radiance nonphotochemical quenching is very high, we assume that energy transfer between PSII units is negligible and that PSII can be regarded as an isolated unit. Regardless of the mechanism involved, a part of the PSII centers is deactivated in the sense that the probability of charge separation or emission of fluorescence upon excitation is very low. The cause could be a disconnection of the antenna, drainage of excitation energy from the antenna or a combination of the two.

The Photosystem Deactivation Model (PDM)

In this model deactivated photosystems absorb light quanta but are not capable of electron transport and fluorescence emission. The fraction of active photosystems is assumed to be ζ , and thus the fraction of deactivated systems is $1-\zeta$. On this basis the photosystem deactivation model (PDM) is formulated. In this model it is as-

sumed that photosystems can be in the following different states:

	Fraction	Fluorescence	Photochemistry
Active photosystems with open reaction centers	ζ		possible
with closed reaction centers	$u \cdot \zeta$	low	
Deactivated photosystems	$(1-u) \cdot \zeta$	high	
	$(1-\zeta)$	none	not possible

For this model the following yield expressions are obtained:

$$\Phi'_F = \zeta \cdot \phi'_F = \zeta [u \cdot k_p / (k_F + k'_D + k_p) + (1-u) \cdot k_p / (k_F + k'_D)], \quad (21)$$

$$\Phi'_p = \zeta \cdot \phi'_p = \zeta [u \cdot k_p / (k_F + k'_D + k_p)]. \quad (22)$$

Here the capital Φ has been used to differentiate the “overall” yield of all photosystems from the lower case ϕ , which is the yield of active photosystems. The following reference values may be introduced:

$$\Phi'_{F0} = \zeta \cdot k_p / (k_F + k'_D + k_p), \quad (23)$$

$$\Phi'_{FM} = \zeta \cdot k_p / (k_F + k'_D). \quad (24)$$

Elimination of the fraction of active open reaction centers (u), from Eqs. (21) and (22), in combination with Eq. (24) leads to the following relation between the “overall” fluorescence and photochemical yield:

$$\Phi'_p = \zeta (1 - \Phi'_F / \Phi'_{FM}) = \zeta (1 - \phi'_F / \phi'_{FM}). \quad (25)$$

This equation is similar to (8) after Genty et al. (1989) except that it includes the fraction of active reaction centers ζ ! This equation implies that the calculated estimates of the photosynthetic quantum yield and electron transport based on the Genty formula (8) do not give the right values if a part of the reaction centers is deactivated ($\zeta < 1$).

Equivalent to Eqs. (12), (15), and (18), we find the following equations, which express the overall quantum yields as a function of the PAR level:

$$\Phi'_p = \zeta \cdot \phi'_p = \zeta \cdot \phi'_{p0} / (1 + r_c \cdot \phi'_{p0} \cdot \text{PAR}), \quad (26)$$

$$\begin{aligned} \Phi'_F / \phi_{F0} &= \zeta \cdot \phi'_F / \phi_{F0} \\ &= \zeta \cdot \{\phi'_{p0} / [(1 - \phi'_{p0}) \phi_{p0}]\} [1 - \phi'_{p0} / (1 + r_c \cdot \phi'_{p0} \cdot \text{PAR})] \end{aligned} \quad (27)$$

with

$$\phi'_{p0} = \phi_{p0} / [1 + b \cdot \text{PAR} \cdot (1 - \phi_{p0} - \phi_{F0})]. \quad (28)$$

Calculation of Photosynthetic Electron Transport Using the PDM

With the PDM the photosynthetic electron transport may be calculated from the fluorescence and PAR values measured with the LEAF-NL instrument. The procedure is as follows. First estimate the (normalized) fluorescence of active photosystems from PAR by means of Eqs. (27) and (28), setting $\zeta = 1$. Then the fraction of active photosystems ζ is obtained as the ratio between the measured fluorescence and the value estimated for active photosystems. (The course of ζ during the drought ex-

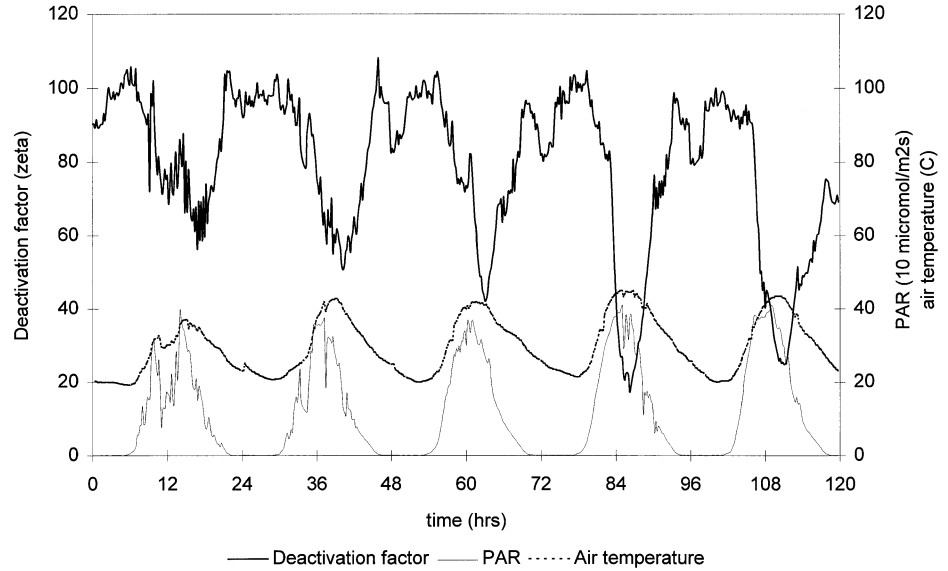


Figure 9. Course of the photosystem deactivation factor (ζ) during the drought experiment. Also the PAR and air temperature are shown.

periment is shown in Figure 9, together with PAR and the air temperature). The photosynthesis yield of active systems (ϕ'_p) is subsequently calculated on the basis of PAR with Eq. (26). Finally the value of the photosynthetic electron transport (E) is obtained with

$$E = \zeta \cdot \phi'_p \cdot \text{PAR} \quad (29)$$

or

$$E = \zeta \cdot \phi'_{p0} \cdot \text{PAR} / (1 + r_c \cdot \phi'_{p0} \cdot \text{PAR}), \quad (30)$$

where ϕ'_{p0} is given by Eq. (28). In the literature electron transport has generally been formulated as the product of ϕ'_p and PAR. This appears to be only correct if no photosystem deactivation occurs ($\zeta=1$) and thus provides only the maximum possible value (E_m):

$$E_m = \phi'_p \cdot \text{PAR}. \quad (31)$$

Comparison of Photosynthetic Electron Transport and CO₂ Assimilation

With the methodology, developed in the previous sections, we have calculated the photosynthetic electron transport on the basis of the fluorescence and radiance measurements obtained with the Laser Environmental Active Fluoro-sensor (LEAF-NL) during the drought and the ozone experiment on small Poplar trees in a gas exchange chamber. These measurements may be compared with the CO₂ exchange measurements that were simultaneously obtained. The results are shown in Figures 10 and 11 for the drought and ozone experiment respectively. In each graph three lines are shown, representing:

- Electron transport (E) according to the PDM using Eq. (30),
- Maximum electron transport (E_m) using Eq. (31),
- Net CO₂ exchange (P_n) based on measurements of the CO₂ concentrations of the inlet and outlet

air of, and the measured air flow rate through, the gas exchange cabinet.

Values of E and E_m are represented on the right axis and P_n on the left axis. Units are not given. An exact, quantitative comparison is not possible for the following reasons:

1. E and E_m are a measure of the gross photosynthesis and in principle represent the sum of photosynthesis and respiration in light.
2. P_n is a measure of net photosynthesis and in principle represents the difference between photosynthesis and respiration in light.
3. E and P_n have been measured in a completely different way. P_n represents the net photosynthesis of all poplars inside the chamber while E represents the gross photosynthesis of only those leaves exposed to the laser beam.

Therefore, an exact correspondence between E and P_n cannot be expected. Major changes in photosynthesis, however, should affect both measurements in a similar way.

The results presented in Figures 10 and 11 show that there is a fair correspondence between E and P_n except for the second day in the graph of the drought experiment. E and P_n both show a skew distribution around noon with lower values in the afternoon than in the morning. During the last 2 days of the drought experiment and the last day of the ozone experiment this is particularly clear. Both display a dramatic decrease of photosynthesis during the afternoon, which is most likely caused by stomatal closure. This correspondence is not observed between E_m and P . The PDM appears to be a suitable tool to trace and estimate major changes in plant photosynthesis.

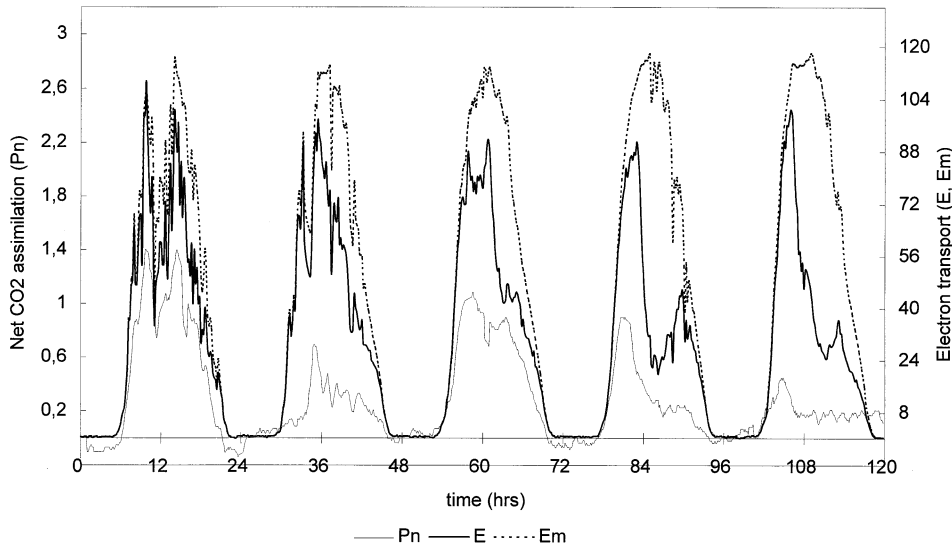


Figure 10. The course of net CO₂ assimilation (P_n) and photosynthetic electron transport derived from the laser-induced chlorophyll fluorescence measurements during the drought experiment, using existing theory (E_m) and the photosystem deactivation model (E). The latter better predicts the (asymmetric) daily course of the CO₂ data, except on the second day.

DISCUSSION

From the fluorescence and PAR data presented in our study it seems that the deactivation mechanism is related to the radiation level. Closer study, however, reveals that there is a phase shift between PAR and ζ . The best empirical relation is found with the average PAR during the five previous hours, as shown in Figure 12:

$$\zeta \cong 0.978 - 0.00164 \cdot \text{PAR}_{5h} \quad (r^2 = 0.81). \quad (32)$$

The reason for this phase shift could be that when a certain radiation level is surpassed, a pool of deactivating substance gradually builds up. The phase shift relative to the irradiation also suggests a relation with the air temperature. The air temperature was measured inside the gas exchange cabinet during the measurements. The empirical relation is shown in Figure 13. It is best approximated by a curve linear regression:

$$\zeta \cong 82.7 + 2.13 T_a - 0.071 T_a^2 \quad (r^2 = 0.73). \quad (33)$$

We do not know, however, if this relation is direct and causal or indirect. The experimental data, however, do suggest that high radiation combined with high leaf temperature induces downregulation of PSII, leading to a strong decline in fluorescence and photochemical yield. The effect is gradually reversed at the end of the day as light and temperature decrease.

Combined effects of light and high temperature have been observed by Schreiber and Berry (1978). They found a strong light-dependent suppression of the minimal fluorescence (ϕ_{F0}) which only occurred at high leaf temperatures. A possible explanation for the combined effect of high radiance and temperature might be found in the temperature dependence of heat dissipation in the PSII antenna. The xanthophyll has been suggested to be involved in the dissipation of excess excitation energy

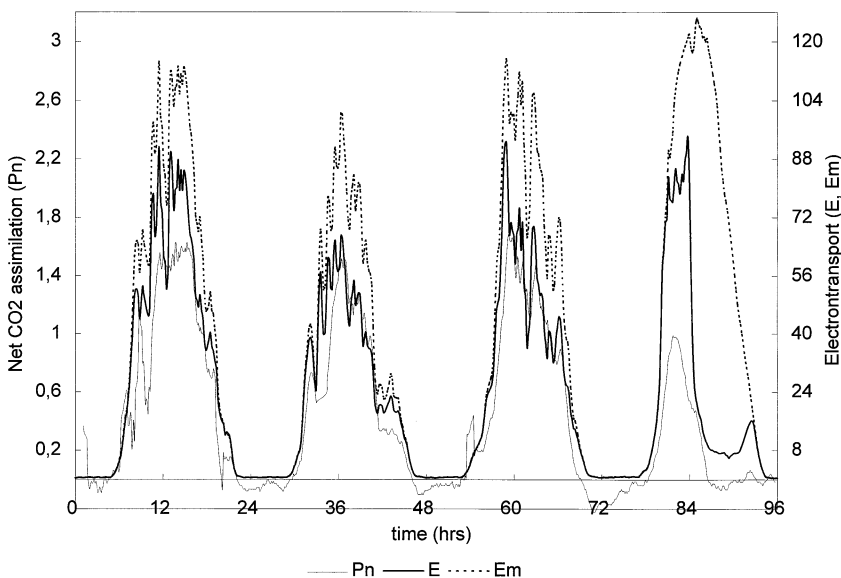


Figure 11. The course of net CO₂ assimilation (P_n) and of the photosynthetic electron transport derived from the laser-induced chlorophyll fluorescence measurements during the ozone fumigation experiment, using existing theory (E_m) and the photosystem deactivation model (E). The latter better predicts the daily course of the CO₂ data, particularly on the last day when the net CO₂ uptake is nil during the afternoon.

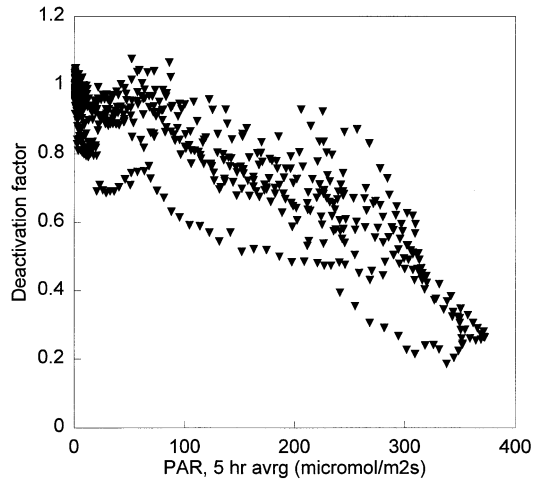
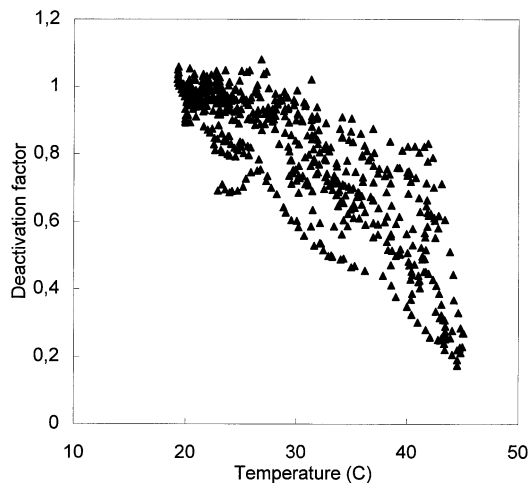


Figure 12. The photosystem deactivation factor plotted as a function of average PAR during the previous 5 h.

(Demmig-Adams and Adams, 1992). This would be mediated by the reversible deepoxidation of violaxanthin to antheraxanthin and zeaxanthin. Zeaxanthin formation in intact leaves has been shown to be temperature dependent with increased rate at higher temperature (Bilger and Björkman, 1991). Barzda et al. (1996) suggest that *in vitro* LHCII aggregation, which is assumed to be involved in the state leading to increased thermal deactivation of excitation energy, may be induced by local heating due to excess light.

The conversion of violaxanthin to zeaxanthin causes a leaf absorption change around 510 nm (Taylor and Björkman, 1990; Gamon et al., 1990). In one of their experiments a sunflower crop, which was suddenly exposed to high solar radiation, showed a simultaneous decrease in (apparent) reflection at 510 nm, 685 nm, and 738 nm.

Figure 13. The photosystem deactivation factor plotted as a function of the air temperature inside the gas exchange cabinet.



The decrease in (apparent) reflection at 685 nm and 738 nm must be due to a decrease in fluorescence, which has emission band maxima at these two wavelengths and is superimposed on the reflection spectrum. The previous indicates that the conversion from violaxanthin to zeaxanthin and the quenching of chlorophyll fluorescence under high light took place simultaneously. This suggests that also in our experiments the strong fluorescence quenching at high light and temperature is related to zeaxanthin formation, which would be mediating the dissipation of excitation energy.

CONCLUSIONS

Our results indicate that reliable estimates of the overall photochemical yield and electron transport cannot always be obtained on the basis of the approach published by Genty et al. (1989). Under our conditions these estimates could be improved considerably by accounting for non-fluorescence (deactivated) photosystems, as proposed in the present article.

Photosystem deactivation is assumed to be a process in which the photosystem loses its ability to emit fluorescence and to transport electrons. The consequent strong quenching of the chlorophyll fluorescence is phase-shifted by several hours relative to the incident radiation. This suggests that light is not the only factor involved.

The present results have an important implication for the application of chlorophyll fluorescence measurements as a remote sensing technique. In remote sensing of vegetation status attention is focused on the occurrence of anomalies in the signal. In the past, photosynthetic stress in vegetation was usually assumed to be expressed as an increase in the fluorescence signal. Our present results show that the opposite may be true! A decrease in CO₂ assimilation was associated with a decrease in chlorophyll fluorescence!

This research was supported by the Netherlands Remote Sensing Board in the framework of the National Remote Sensing Programme. The authors would like to thank Mrs. Ria van den Noort for growing the poplar plants.

REFERENCES

- Barzda, V., Istokovics, A., Simidjiev, I., and Garab, G. (1996), Structural flexibility of chiral macroaggregates of light-harvesting chlorophyll a/b pigment-protein complexes. Light-induced reversible structural changes associated with energy dissipation. *Biochemistry* 35(27):8981–8985.
- Bilger, W., and Björkman, O. (1991), Temperature dependence of violaxanthin deepoxidation and nonphotochemical fluorescence quenching in intact leaves of *Gossypium hirsutum* L. and *Malva parviflora* L., *Planta* 184:226–234.
- Björkman, O., and Demmig-Adams, B. (1995), Regulation of photosynthetic light energy capture, conversion and dissipation.

- tion in leaves of higher plants. In *Ecophysiology of Photosynthesis* (E.-D. Schulze and M. M. Caldwell, Eds.), Springer-Verlag, Heidelberg, pp. 17–47.
- Cecchi, G., Mazzinghi, P., Pantani, L., Valentini, R., Tirelli, D., and De Angelis, P. (1994), Remote sensing of chlorophyll-a fluorescence of vegetation canopies: 1. Near and far field measurement techniques. *Remote Sens. Environ.* 47:18–28.
- Demmig, B., and Björkman, O. (1987), Comparison of the effect of excessive light on chlorophyll fluorescence (77K) and photon yield of O₂ evolution in leaves of higher plants. *Planta* 171:171–184.
- Demmig-Adams, B., and Adams, W. W., III (1992), Photoprotection and other responses of plants to high light stress. *Annu. Rev. Plant Physiol. Plant Mol. Biol.* 43:599–626.
- Gamon, J. A., Field, C. B., Bilger, W., Björkman, O., Fredeen, A. L., and Penuelas, J. (1990), Remote sensing of the xanthophyll cycle and chlorophyll fluorescence in sunflower leaves and canopies. *Oecologia* 85:1–7.
- Genty, B., Briantais, J., and Baker, N. L. (1989), The relationship between the quantum yield of photosynthetic electron transport and quenching of chlorophyll fluorescence. *Biochim. Biophys. Acta* 990:87–92.
- Günther, K. P., Lüdeker, W., and Dahn, H. G. (1991), Design and testing of a spectral-resolving fluorescence LIDAR system for Remote Sensing of vegetation. In *5th International Colloquium on Physical Measurements and Signatures in Remote Sensing*, Courchevel, ESA SP-319, pp. 723–726 (2 Vols.).
- Günther, K. P., Dahn, H. G., and Lüdeker, W. (1994), Remote sensing of vegetation status by laser-induced fluorescence. *Remote Sens. Environ.* 47:10–17.
- Lichtenthaler, H. K., Stober, F., and Lang, M. (1992), The nature of different laser-induced fluorescence signatures of plants. *EARSeL Adv. Remote Sens.* 1:(2):20–32.
- Lipucci di Paola, M., Mazzinghi, P., Pardossi, A., and Vernieri P. (1992), Vegetation monitoring of chilling stress by chlorophyll fluorescence ratio. *EARSeL Adv. Remote Sens.* 1(2):2–6.
- Methy, M., Olioso, A., and Trabaud, L. (1994), Chlorophyll fluorescence as a tool for management of plant resources. *Remote Sens. Environ.* 47:2–9.
- Mohammed, G. H., Binder, W. D., and Gillies, S. L. (1995), Chlorophyll fluorescence: a review of its practical forestry applications and instrumentation. *Scand. J. For. Res.* 10: 383–410.
- Moya, I., Goulas, Y., Briantais, J. M., Camenen, L., Gorbunov, M., and Cerovic, Z. G. (1995), Remote Sensing of diurnal changes of chlorophyll fluorescence lifetime effects of water deficit on maize. In *Proceedings of the International Colloquium on Photosynthesis and Remote Sensing* (G. Guyot, Ed.), 28–30 August, Montpellier, France, pp. 45–54, EARSeL, Paris and INRA, Avignon.
- Pieters, G. A., and Van den Noort, M. E. (1985), Leaf area coefficient of some *Populus euramericana* cultivars grown at various irradiances and NO₃ supply. *Photosynthetica* 19: 188–193.
- Poulet, P., Cahen, D., and Malkin, S. (1983), Photoacoustic detection of photosynthetic oxygen evolution from leaves. Quantitative analysis by phase and amplitude measurements. *Biochim. Biophys. Acta* 724:433–446.
- Rosema, A., and Verhoef, W. (1991), Modeling of fluorescence light–canopy interaction. In *Proceedings of the 5th International Colloquium Physical Measurements and Signatures in Remote Sensing*, Courchevel, France, 14–18 January, ESA SP-319, pp. 743–748.
- Rosema, A., and Zahn H. (1997), Laser pulse energy requirements for remote sensing of chlorophyll fluorescence. *Remote Sens. Environ.* 62(1):101–108.
- Rosema, A., Cecchi, G., Pantani, L., et al. (1988), Results of the LIFT project: air pollution effects on the fluorescence of Douglas fir and poplar. In *Applications of Chlorophyll Fluorescence* (H. K. Lichtenthaler, Ed.), Kluwer Academic Dordrecht, pp. 307–318.
- Rosema, A., Verhoef, W., Schroote, J., and Snel, J.F.H. (1991), Simulating fluorescence light–canopy interaction in support of laser-induced fluorescence measurements. *Remote Sens. Environ.* 37:117–130.
- Rosema, A., Schroote, J., Snel, J. H. F., Verhoef, W., and Mertens, L. (1992), LEAF/Research Final Report. Report no. 91-16, Netherlands Remote Sensing Board, Delft.
- Rosema, A., Lucassen, G. W., Schroote, J., et al. (1994a), LEAF/Research 1991, Final Report, Report No. 93-19, Netherlands Remote Sensing Board, Delft, April, 67 pp.
- Rosema, A., Lucassen, G. W., Steingröver, G. W., and Snel, J. F. H. (1994b), Laser-induced fluorescence of Douglas fir and its relation to photosynthesis. In LEAF 1993—Final Report, Report No. 94-03, Netherlands Remote Sensing Board, Delft, July, 103 pp.
- Schmuck, G., and Moya, I. (1994), Time-resolved chlorophyll fluorescence spectra of intact leaves. *Remote Sens. Environ.* 47:72–76.
- Schreiber, U., and Berry, J. A. (1977), Heat-induced changes of chlorophyll fluorescence in intact leaves correlated with damage to the photosynthetic apparatus. *Planta* 136:233–238.
- Srivastava, A., Greppin, H., and Strasser, R. J. (1995), The steady state chlorophyll-a fluorescence exhibits *in vivo* an optimum as function of the light intensity which reflects the physiological state of the plant. *Plant Cell Physiol.* 36(5):839–848.
- Stober, C., Lang, M., and Lichtenthaler, H. K. (1994), Blue, green and red fluorescence emission signatures of green etiolated and white leaves. *Remote Sens. Environ.* 47:65–71.
- Taylor, S. S., and Björkman, O. (1990), LEAF xanthophyll content and composition in sun and shade determined by HPLC. *Photosynthesis Res.* 23:331–343.
- Valentini, R., Cecchi, G., Mazzinghi, P., et al. (1994), Remote sensing of chlorophyll-a fluorescence of vegetation canopies: 2. Physiological significance of fluorescence signal in response to environmental stress. *Remote Sens. Environ.* 47:29–35.
- Van Hove, L. W. A. (1989), The mechanism of NH₃ and SO₂ uptake by leaves and its physiological effects, Ph.D. thesis, Agricultural University Wageningen, The Netherlands.
- Van Kooten, O., and J. F. H. Snel (1990), The use of chlorophyll fluorescence nomenclature in plant stress physiology. *Photosynthesis Res.* 25:147–150.